

Gut flora metabolism of phosphatidylcholine promotes cardiovascular disease

Zeneng Wang^{1,2}, Elizabeth Klipfell^{1,2}, Brian J. Bennett³, Robert Koeth¹, Bruce S. Levison^{1,2}, Brandon DuGar¹, Ariel E. Feldstein^{1,2}, Earl B. Britt^{1,2}, Xiaoming Fu^{1,2}, Yoon-Mi Chung^{1,2}, Yuping Wu⁴, Phil Schauer⁵, Jonathan D. Smith^{1,6}, Hooman Allayee⁷, W. H. Wilson Tang^{1,2,6}, Joseph A. DiDonato^{1,2}, Aldons J. Lusis³ & Stanley L. Hazen^{1,2,6}

Metabolomics studies hold promise for the discovery of pathways linked to disease processes. Cardiovascular disease (CVD) represents the leading cause of death and morbidity worldwide. Here we used a metabolomics approach to generate unbiased small-molecule metabolic profiles in plasma that predict risk for CVD. Three metabolites of the dietary lipid phosphatidylcholine—choline, trimethylamine *N*-oxide (TMAO) and betaine—were identified and then shown to predict risk for CVD in an independent large clinical cohort. Dietary supplementation of mice with choline, TMAO or betaine promoted upregulation of multiple macrophage scavenger receptors linked to atherosclerosis, and supplementation with choline or TMAO promoted atherosclerosis. Studies using germ-free mice confirmed a critical role for dietary choline and gut flora in TMAO production, augmented macrophage cholesterol accumulation and foam cell formation. Suppression of intestinal microflora in atherosclerosis-prone mice inhibited dietary-choline-enhanced atherosclerosis. Genetic variations controlling expression of flavin monooxygenases, an enzymatic source of TMAO, segregated with atherosclerosis in hyperlipidaemic mice. Discovery of a relationship between gut-flora-dependent metabolism of dietary phosphatidylcholine and CVD pathogenesis provides opportunities for the development of new diagnostic tests and therapeutic approaches for atherosclerotic heart disease.

The pathogenesis of CVD includes genetic and environmental factors. A known environmental risk factor for the development of CVD is a diet rich in lipids. A relationship between blood cholesterol and triglyceride levels and cardiovascular risk is well established. However, less is known about the role of the third major category of lipids, phospholipids, in atherosclerotic heart disease pathogenesis.

Another potential yet controversial environmental factor in the development or progression of atherosclerotic heart disease is inflammation due to infectious agents. Some studies have reported associations between coronary disease and pathogens such as cytomegalovirus (CMV), *Helicobacter pylori*, and *Chlamydia pneumoniae*^{1–4}. However, prospective randomized trials with antibiotics in humans have thus far failed to demonstrate cardiovascular benefit^{5–7} and studies with germ-free hyperlipidaemic mice confirm that infectious agents are not necessary for murine atherosclerotic plaque development⁸. Although a definite cause-and-effect relationship between a bacterial or viral pathogen and atherosclerosis in humans has not yet been established, the prospect of a role for microbes in atherosclerosis susceptibility remains enticing.

The intestinal microbiota ('gut flora'), comprised of trillions of typically non-pathogenic commensal organisms, serve as a filter for our greatest environmental exposure—what we eat. Gut flora have an essential role, aiding in the digestion and absorption of many nutrients⁹. Animal studies have recently shown that intestinal microbial communities can influence the efficiency of harvesting energy from diet, and consequently influence susceptibility to obesity¹⁰. Metabolomics studies of inbred mouse strains have also recently shown that gut microbiota may have an active role in the development of complex metabolic abnormalities, such as susceptibility to insulin resistance and non-alcoholic fatty liver disease¹¹. A link between gut-flora-dependent

phospholipid metabolism and atherosclerosis risk through generation of pro-atherosclerotic metabolites has not yet been reported.

Metabolomics studies identify markers of CVD

In initial studies we sought to discover unbiased small-molecule metabolic profiles in plasma that predict increased risk for CVD. An initial 'Learning Cohort' was used comprising plasma from stable patients undergoing elective cardiac evaluation who subsequently experienced a heart attack (myocardial infarction), stroke or death over the ensuing three-year period versus age- and gender-matched subjects who did not. Liquid chromatography with on-line mass spectrometry (LC/MS) analysis of plasma was performed to define analytes associated with cardiac risk as described in Methods. Of an initial 2,000+ analytes monitored, 40 met all acceptability criteria within the Learning Cohort. Subsequent studies within an independent 'Validation Cohort' led to identification of 18 analytes that met acceptability criteria in both Learning and Validation Cohorts (Fig. 1a, b, Supplementary Fig. 1a and Supplementary Table 1).

The structural identity of the 18 small molecules in plasma, the levels of which track with cardiac risks, was not known, as the compounds were screened on the basis of retention time and mass-to-charge ratio (*m/z*) when analysed by LC/MS. Among the 18 analytes, those with *m/z* 76, 104 and 118 demonstrated significant ($P < 0.001$) correlations among one another, suggesting a potential relationship via a common biochemical pathway (Supplementary Fig. 1b). We therefore initially sought to structurally define these three analytes.

Phosphatidylcholine metabolites are linked to CVD

The candidate compound in plasma with an *m/z* of 76 associated with CVD risks was isolated and unambiguously identified as TMAO using

¹Department of Cell Biology, Cleveland Clinic, Cleveland, Ohio 44195, USA. ²Center for Cardiovascular Diagnostics and Prevention, Cleveland Clinic, Cleveland, Ohio 44195, USA. ³Department of Medicine/Division of Cardiology, BH-307 Center for the Health Sciences, University of California, Los Angeles, California 90095, USA. ⁴Department of Mathematics, Cleveland State University, Cleveland, Ohio 44115, USA. ⁵Bariatric and Metabolic Institute, Cleveland Clinic, Cleveland, Ohio 44195, USA. ⁶Department of Cardiovascular Medicine, Cleveland Clinic, Cleveland, Ohio 44195, USA. ⁷Department of Preventive Medicine and Institute for Genetic Medicine, Keck School of Medicine, University of Southern California, Los Angeles, California 90089, USA.

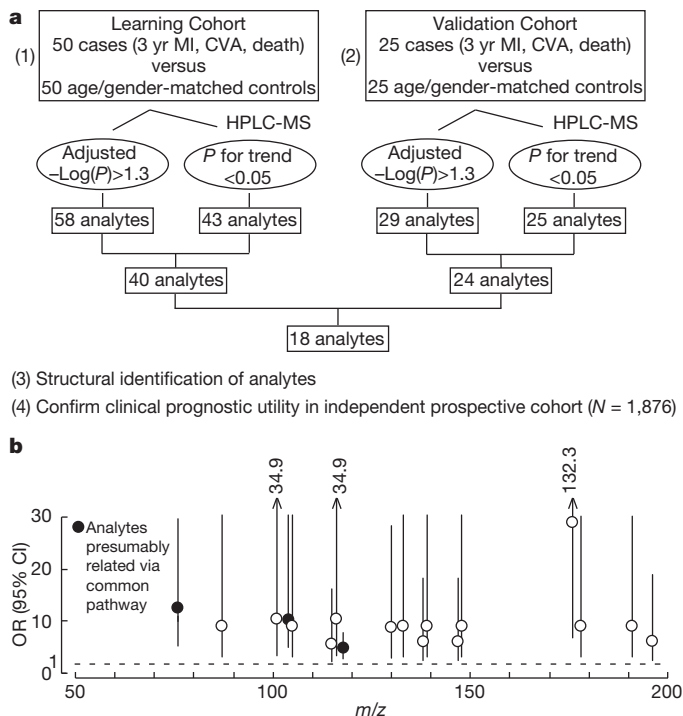


Figure 1 | Strategy for metabolomics studies to identify plasma analytes associated with cardiovascular risk. **a**, Overall schematic to identify plasma analytes associated with cardiac risk over the ensuing 3-year period. CVA, cerebrovascular accident; HPLC, high-performance liquid chromatography; MI, myocardial infarction. **b**, Odds ratio (OR) and 95% confidence intervals (CI) of incident (3-year) risk for MI, CVA or death of the 18 plasma analytes that met all selection criteria in both Learning and Validation Cohorts; odds ratio and 95% confidence intervals shown are for the highest versus lowest quartile for each analyte. Filled circles represent the analytes ($m/z = 76, 104, 118$) focused on in this study. m/z , mass to charge ratio.

multinuclear nuclear magnetic resonance (NMR), multi-stage mass spectrometry (MS^n), liquid chromatography with tandem mass spectrometry (LC/MS/MS) and gas chromatography with tandem mass spectrometry (GC/MS/MS) after multiple derivatization strategies (see Methods, Supplementary Figs 2a–d, and Supplementary Table 2). TMAO, an oxidation product of trimethylamine (TMA), is a relatively common metabolite of choline in animals^{12,13}. Foods rich in the lipid phosphatidylcholine (PC, also called lecithin), which predominantly include eggs, milk, liver, red meat, poultry, shell fish and fish, are believed to be the major dietary sources for choline, and hence TMAO production¹⁴. Briefly, initial catabolism of choline and other trimethylamine-containing species (for example, betaine) by intestinal microbes forms the gas TMA¹⁵, which is efficiently absorbed and rapidly metabolized by at least one member of the hepatic flavin monooxygenase (FMO) family of enzymes, FMO3, to form TMAO^{15,16}. Identification of the plasma analyte associated with CVD risk with an m/z of 76 as TMAO therefore indicated that the plasma analyte with an m/z of 104 might be choline. Further, these results also indicated that the plasma analyte with an m/z of 118 associated with CVD might be related to PC (choline) metabolism.

To test the hypothesis that the plasma analytes with m/z 76 (TMAO), 104 and 118 might all be derived from the major dietary lipid PC, mice were fed egg-yolk PC (through oral gavage) and plasma levels of analytes over time were monitored. In both male and female mice, analytes with the same m/z (76, 104 and 118) and the same retention times as the corresponding analytes of interest observed in human plasma all increased after oral PC feeding (Supplementary Fig. 3a, b), strongly indicating that the m/z 104 analyte was choline, and the analyte at m/z 118 was derived from PC. Confirmation that the plasma analyte (m/z 104) associated with CVD risk was choline was achieved by

MS^n , LC/MS/MS and GC/MS/MS after multiple derivatization strategies (Supplementary Fig. 4a–d and Supplementary Table 3).

We next studied the plasma analyte with m/z 118. We proposed that the analyte was either betaine or one of several potential methylated metabolites of choline (see Supplementary Fig. 5a for structures and strategy for discrimination among these isomers). To distinguish between these species, and explore a role for intestinal generation of the various metabolites, different isotopically labelled choline precursors were administered to mice either through an oral (gavage) or a parenteral (intraperitoneal, i.p.) route. The observed m/z of new isotopically labelled analytes at the appropriate retention times identified in plasma after these isotope tracer studies are summarized in Fig. 2a. Oral administration of non-labelled choline resulted in time-dependent increases in plasma levels of analytes with m/z 76, 104 and 118, consistent with TMAO, choline and either betaine or a methylated choline species (Supplementary Fig. 6a). Use of selectively deuterated choline species at either the trimethylamine moiety (d9 isotopomer) or the ethyl moiety (d4 isotopomer) unambiguously confirmed the m/z 118 analyte as betaine (Fig. 2a and Supplementary Fig. 6b). Further confirmation was acquired by observing the same retention time in LC/MS and an identical collision-induced dissociation (CID) mass spectrum (Supplementary Fig. 5b). Moreover, supplementation of PC or choline isotopomers via gavage or i.p. injection showed an absolute requirement for the oral route in TMAO production, whereas betaine production from PC or choline was formed via both oral and i.p. routes (Fig. 2 and Supplementary Fig. 7a).

Gut flora is needed to form TMAO from dietary PC

Intestinal microflora have a role in TMAO formation from dietary free choline¹³. We therefore proposed that commensal organisms (gut flora) might also have an obligate role in TMAO formation from dietary PC. To test this, deuterated PC was synthesized whereby the choline-methyl groups were deuterium labelled (that is, d9-PC) and

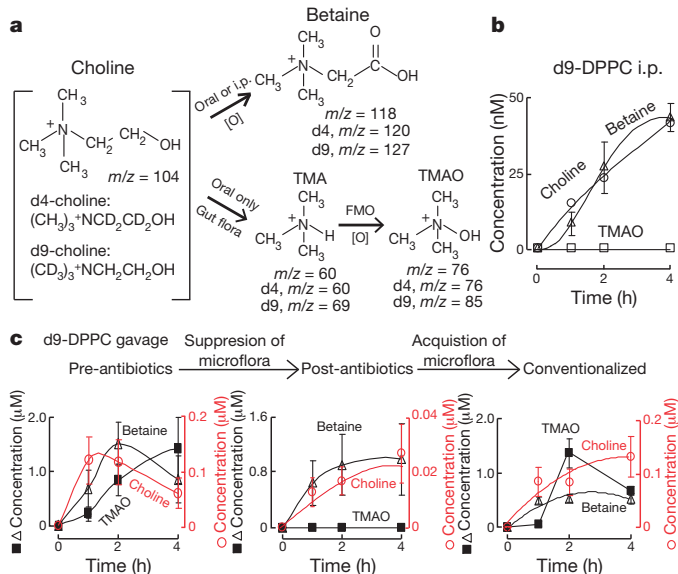


Figure 2 | Identification of metabolites of dietary PC and an obligatory role for gut flora in generation of plasma analytes associated with CVD risk.

a, Summary schematic indicating structure of metabolites and routes (oral or i.p.) of formation observed in choline challenge studies in mice using the indicated isotope-labelled choline. The m/z in plasma observed for the isotopomers of the choline metabolites are shown. **b**, Plasma levels of d9 metabolites after i.p. challenge with d9(trimethyl)-dipalmitoylphosphatidylcholine (d9-DPPC). **c**, d9-TMAO production after oral d9-DPPC administration in mice, following suppression of gut flora with antibiotics (3 weeks), and then following placement (4 weeks) into conventional cages with non-sterile mice ('conventionalized'). Data are presented as mean \pm standard error (s.e.) from four independent replicates.

used as isotope tracer for feeding studies. When mice were fed through oral gavage with d9-PC, the time-dependent appearance of the anticipated d9 isotopomer of TMAO was observed in plasma (Fig. 2c). Interestingly, pre-treatment of mice with a three-week course of broad-spectrum antibiotics to suppress intestinal flora completely suppressed the appearance of d9-TMAO in plasma after oral d9-PC administration (Fig. 2c). A similar pattern was observed after oral administration of d9-choline to mice, with d9-TMAO produced in untreated mice, but not in the same mice after a 3-week course of broad-spectrum antibiotics (Supplementary Fig. 7b), or in germ-free mice born sterilely by Caesarean section (Supplementary Fig. 7c). In a final series of studies, mice with suppressed intestinal microflora after antibiotics were placed in conventional cages with normal (non-germ-free) mice to permit intestinal colonization with microbes. After four weeks, repeat oral d9-PC challenge of the now 'conventionalized' mice resulted in readily detectable plasma levels of d9-TMAO (Fig. 2c). Similar results were observed after conventionalization of germ-free mice and oral d9-choline (Supplementary Fig. 7c). Collectively, these results show an obligate role for intestinal microbiota in the generation of TMAO from the dietary lipid PC. They also reveal the following metabolic pathway for dietary PC producing TMAO: PC → choline → TMA → TMAO.

Dietary PC metabolites predict CVD risk

We next sought to independently confirm the prognostic value of monitoring fasting plasma levels of TMAO, choline and betaine in a large independent clinical cohort distinct from subjects examined in both the Learning and Validation Cohorts. Stable subjects ($N = 1,876$) undergoing elective cardiac evaluations were enrolled. Clinical, demographic and laboratory characteristics of the cohort are provided in Supplementary Table 4a. Fasting plasma levels of TMAO, choline and betaine were quantified by LC/MS/MS using methods specific for each analyte (Supplementary Fig. 8). Increasing levels of choline, TMAO and betaine were all observed to show dose-dependent associations with the presence of CVD (Fig. 3a–c) and multiple individual CVD phenotypes including peripheral artery disease (PAD), coronary artery disease (CAD), and history of myocardial infarction (see Supplementary Table 5a–d for multilogistic regression models, and Supplementary Table 5e for Somers' Dxy correlation). The associations between increased risk of all CVD phenotypes monitored and elevated systemic levels of the three PC metabolites held true after adjustments for traditional cardiac risk factors and medication usage (Fig. 3a–c and Supplementary Table 5a–e).

Dietary choline or TMAO promotes atherosclerosis

We next investigated whether the strong associations noted between plasma levels of the dietary PC metabolites and CVD risk reflected some hidden underlying pro-atherosclerotic mechanism. Atherosclerosis-prone mice (C57BL/6J *Apoe*^{-/-}) at time of weaning were placed on either normal chow diet (contains 0.08–0.09% total choline, wt/wt) or normal chow diet supplemented with intermediate (0.5%) or high amounts of additional choline (1.0%) or TMAO (0.12%). At 20 weeks of age increased total aortic root atherosclerotic plaque area was noted in both male and female mice on diets supplemented with either choline or TMAO (Fig. 3d and Supplementary Fig. 9a). Analysis of plasma levels of choline and TMAO in each of the dietary arms showed nominal changes in plasma levels of choline, but significant increases of TMAO in mice receiving either choline or TMAO supplementation (Supplementary Fig. 10). Parallel examination of plasma cholesterol, triglycerides, lipoproteins, glucose levels and hepatic triglyceride content in the mice failed to show significant increases that could account for the enhanced atherosclerosis (Supplementary Table 6 and Supplementary Fig. 11). Interestingly, all dietary groups of mice revealed a significant positive correlation between plasma levels of TMAO and atherosclerotic plaque size (Fig. 3e and Supplementary Fig. 9b). Of note, plasma TMAO levels observed within the female mice (which

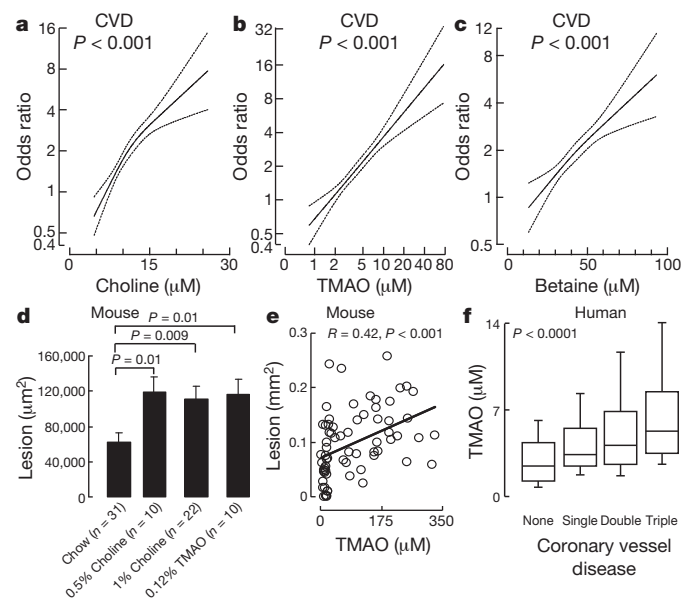


Figure 3 | Plasma levels of choline, TMAO and betaine are associated with atherosclerosis risks in humans and promote atherosclerosis in mice.

a–c, Spline models of the logistic regression analyses reflecting risk of CVD (with 95% CI) according to plasma levels of choline, TMAO and betaine in the entire cohort ($n = 1,876$ subjects). d, Comparison in aortic lesion area among 20-week-old female C57BL/6J *Apoe*^{-/-} mice fed with chow diet supplemented with the indicated amounts (wt/wt) of choline or TMAO from time of weaning (4 weeks). e, Relationship between plasma TMAO levels and aortic lesion area. f, Relationship between fasting plasma levels of TMAO versus CAD burden among subjects ($N = 1,020$). Boxes represent 25th, 50th and 75th percentile, and whiskers 5th and 95th percentile plasma levels. Single, double and triple coronary vessel disease refers to number of major coronary vessels demonstrating $\geq 50\%$ stenosis on diagnostic coronary angiography.

get enhanced atherosclerosis relative to their male counterparts), even on normal chow diet, were significantly higher than those observed among male mice (Supplementary Fig. 10). No significant gender differences in plasma levels of TMAO were observed in humans ($P = 0.47$); however, a clear dose–response relationship was observed between TMAO levels and clinical atherosclerotic plaque burden in subjects undergoing coronary angiography (Fig. 3f).

Hepatic FMOs, TMAO and atherosclerosis

Hepatic FMO3 is a known enzymatic source for TMAO in humans, based on the recent recognition of the aetiology of an uncommon genetic disorder called trimethylaminuria (also known as fish malodour syndrome)^{15,17}. Subjects with this metabolic condition have impaired capacity to convert TMA, which smells like rotting fish, into TMAO, an odourless stable oxidation product¹⁷. We therefore sought to identify possible sources of genetic regulation and the role of *Fmo3* in atherosclerosis using integrative genetics in mice¹⁸. Expression levels of *Fmo3* were determined by microarray analysis in the livers of mice from an F2 intercross between atherosclerosis-prone C57BL/6J *Apoe*^{-/-} mice and atherosclerosis-resistant C3H/HeJ *Apoe*^{-/-} mice and compared with quantitative measures of atherosclerosis. The expression level of *Fmo3* showed marked differences between genders (females $>1,000$ fold higher than in males). Significant positive correlations were readily found between hepatic *Fmo3* expression and atherosclerotic lesions (Fig. 4a, Supplementary Fig. 12, top row, and Supplementary Fig. 13). Interestingly, a highly significant negative correlation with plasma high-density lipoprotein (HDL) cholesterol levels was noted in both male and female mice (Fig. 4b and Supplementary Fig. 12, middle row). Further, plasma levels of the PC metabolite TMAO showed a significant positive correlation with hepatic *Fmo3* expression level in mice (Fig. 4c and Supplementary Fig. 12, bottom row).

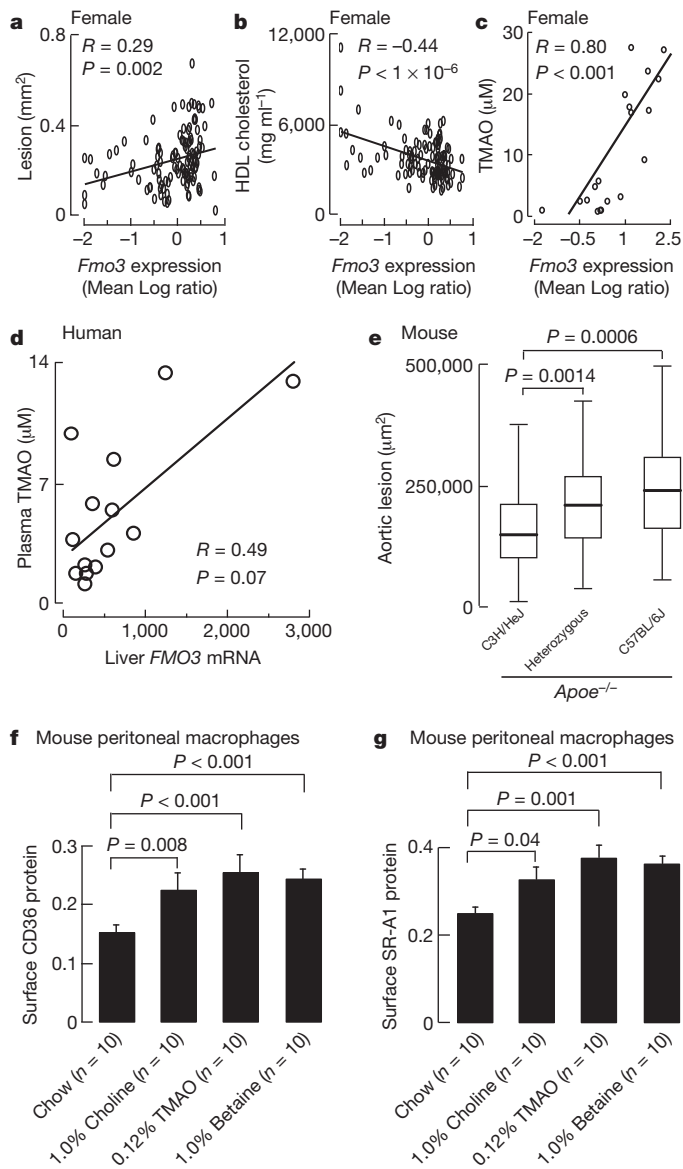


Figure 4 | Hepatic *Fmo* genes are linked to atherosclerosis and dietary PC metabolites enhance macrophage scavenger receptor expression.

a–c, Correlation between hepatic *Fmo3* expression and aortic lesion, plasma HDL cholesterol and TMAO in female mice from the F2 intercross between atherosclerosis-prone C57BL/6J *Apoe*^{-/-} and atherosclerosis-resistant C3H/HeJ *Apoe*^{-/-} mice. **d**, Correlation between human hepatic *FMO3* expression and plasma TMAO. **e**, Effect of *Fmo3* genotype (SNP rs3689151) on aortic sinus atherosclerosis in male mice from the C57BL/6J *Apoe*^{-/-} and C3H/HeJ *Apoe*^{-/-} F2 intercross. **f, g**, Quantification of scavenger receptor CD36 and SR-A1 surface protein levels in macrophages harvested from C57BL/6J mice (13 week) after three weeks of standard chow versus chow supplemented with the indicated amounts (wt/wt) of choline, TMAO or betaine. Data are presented as mean \pm s.e. from the indicated numbers of mice in each group.

FMO3 is one member of a family of FMO enzymes, the majority of which are physically located as a cluster of genes on chromosome 1 in both humans and mice. The various FMOs share sequence homology and overlapping substrate specificities. Further, although rare mutations in or near the *FMO3* gene have been identified in individuals with trimethylaminuria¹⁹, the impact of these mutations on other *FMO* genes remains unknown. Examination of the hepatic expression levels of the various *FMO* genes revealed that many are highly correlated with each other in both mice and humans (Supplementary Table 7). Examination of hepatic expression levels of additional *Fmo* genes in mice from the atherosclerosis F2 intercross revealed that multiple *Fmo* genes are

significantly correlated with aortic lesion formation, HDL cholesterol concentrations and plasma TMAO levels (Supplementary Figs 14–16), suggesting that several members of the FMO family of enzymes may participate in atherosclerosis and the PC \rightarrow TMAO metabolic pathway. To explore the relationship between hepatic FMOs and plasma TMAO levels in humans, paired samples of liver and plasma from subjects undergoing elective liver biopsy were examined. Among all of the human *FMO* genes monitored, only a trend towards positive association was noted between hepatic expression of *FMO3* and plasma TMAO levels (Fig. 4d and Supplementary Fig. 17).

Next, we focused on the genetic regulation of hepatic *Fmo3* expression (and other *Fmo* genes) using expression quantitative trait locus (eQTL) analyses in the F2 mouse intercross. The eQTL plot for *Fmo3* messenger RNA levels is shown in Supplementary Fig. 18, and demonstrates a strongly suggestive *cis* locus (lod score = 5.9) on mouse chromosome 1 at 151 Mb. *Fmo3* (and several other *Fmo* genes) is located at 164.8 Mb in a region identified as non-identical by descent between C3H/HeJ and C57BL/6 (<http://mouse.cs.ucla.edu/perlegen/>). This region is just distal to the 95% confidence interval of a previously reported murine atherosclerosis susceptibility locus²⁰. Examining the effect of the closest single-nucleotide polymorphism (SNP) to *Fmo3* (rs3689151) as a function of alleles inherited from either parental strain indicated a strong effect on atherosclerosis in both genders of the F2 mice (Kruskal–Wallis test, $P < 1.0 \times 10^{-6}$). Bonferroni corrected pairwise comparisons indicated a dose-dependent significant increase in atherosclerosis in F2 mice heterozygous or homozygous for the C57BL/6J allele (Fig. 4e). Although the resolution on average for an F2 intercross of this size is in excess of 20 Mb and thus does not provide ‘gene-level’ resolution, these data show that the locus encompassing the *Fmo* gene cluster on chromosome 1 is associated with atherosclerotic lesion size. Collectively, these results indicate that: (1) hepatic expression levels of multiple *Fmo* genes are linked to plasma TMAO levels in mice; (2) hepatic expression levels of multiple *Fmo* genes are associated with both the extent of aortic atherosclerosis and HDL cholesterol levels in mice; (3) hepatic expression levels of *FMO3* indicate an association with plasma TMAO levels in humans; and (4) a genetic locus containing the *Fmo* gene cluster on chromosome 1 in mice has a strong effect on atherosclerosis.

Diet and gut flora alter macrophage phenotype

To explore potential mechanisms through which dietary choline and its metabolites might exert their pro-atherosclerotic effects, C57BL/6J *Apoe*^{-/-} mice at time of weaning were placed on a normal chow diet supplemented with either choline, TMAO or betaine (for >3 weeks). Both mRNA levels (Supplementary Fig. 19) and surface protein levels (Fig. 4f, g and Supplementary Fig. 20) of two macrophage scavenger receptors implicated in atherosclerosis, CD36 and SR-A1, were then determined in peritoneal macrophages. Relative to normal chow diet, mice supplemented with either choline, TMAO or betaine all showed enhanced macrophage levels of CD36 and SR-A1. We next examined the impact of dietary choline and gut flora on endogenous formation of cholesterol-laden macrophage foam cells, one of the earliest cellular hallmarks of the atherosclerotic process. Hyperlipidaemic C57BL/6J *Apoe*^{-/-} mice were fed diets with defined levels of choline as follows: (1) ‘control’ (0.07–0.08%, wt/wt), which is similar to the choline content of normal chow (0.08–0.09%); versus (2) high ‘choline’, corresponding to a >10-fold higher level of choline (1.0%, wt/wt) than normal chow. Concomitantly, half of the mice were administered broad-spectrum antibiotics for 3 weeks to suppress intestinal microflora, which was confirmed by the reduction of plasma TMAO levels by >100-fold (plasma TMAO concentrations in groups receiving antibiotics were <100 nM). Whereas mice on the control diet showed modest evidence of endogenous macrophage foam cell formation, as indicated by Oil-red-O staining of peritoneal macrophages, mice on the 1% choline supplemented diet showed markedly enhanced lipid-laden macrophage development (Fig. 5a). In contrast, suppression of intestinal flora

significantly inhibited dietary-choline-induced macrophage foam cell formation (Fig. 5a, b). These results were confirmed by microscopic quantification of endogenous foam cell levels (Fig. 5b) and analytical quantification of the cholesterol content of recovered macrophages (Fig. 5c). Histopathology and biochemical studies of livers recovered from these mice showed no evidence of steatosis (Supplementary Fig. 21). Parallel analyses of plasma PC metabolites also demonstrated no significant changes in choline or betaine levels between the different dietary groups, and significant increases of plasma TMAO levels only in mice on the high-choline diet in the absence of antibiotics (males,

control versus choline diet, $2.5 \pm 0.1 \mu\text{M}$ versus $28.3 \pm 2.4 \mu\text{M}$, $P < 0.001$; for females, control versus choline diet, $4.0 \pm 0.5 \mu\text{M}$ versus $158.6 \pm 32.9 \mu\text{M}$, $P < 0.001$).

Gut flora promote diet-induced atherosclerosis

In additional studies we sought to test whether gut flora is involved in dietary choline-induced atherosclerosis. At the time of weaning (4 weeks old), atherosclerosis-prone C57BL/6J *Apoe*^{-/-} mice were placed on either a control diet ($0.08 \pm 0.01\%$, wt/wt, choline) or a diet supplemented with 1% choline (wt/wt, choline diet). Half of the mice were also treated with broad-spectrum antibiotics to suppress intestinal microflora. Serial plasma measurements confirmed suppression of TMAO levels to virtually non-detectable levels ($<100 \text{ nM}$) throughout the duration of the study. At 20 weeks of age, mice were killed and aortic root lesion development was quantified. In the absence of antibiotics (that is, with preserved intestinal microflora), choline supplementation augmented atherosclerosis in both male and female mice nearly three-fold (Figs 5d–f). In contrast, suppression of intestinal flora completely inhibited dietary choline-mediated enhancement in atherosclerosis (Figs 5d–f). Aortic macrophage content and scavenger receptor CD36 immunoreactive surface area within aortic lesions were markedly increased in mice on the high-choline diet, but not when intestinal microflora was suppressed with antibiotic treatment (Fig. 5g, h and Supplementary Figs 22, 23). Both histopathological and biochemical examination of liver sections from mice showed no evidence of steatosis or altered neutral lipid (triglyceride or cholesterol/cholesterol ester) levels on either diet in the absence or presence of antibiotics (Supplementary Fig. 21 and Supplementary Table 8). Finally, the structural specificity of PC metabolites in promoting a pro-atherogenic macrophage phenotype was examined. Mice fed diets supplemented with trimethylamine species (choline or TMAO) showed increased peritoneal macrophage cholesterol content and raised plasma levels of TMAO. In contrast, dietary supplementation with the choline analogue 3,3-dimethyl-1-butanol (DMB), where the quaternary amine nitrogen of choline is replaced with a carbon, resulted in no TMAO increase and no increased cholesterol in macrophages (Supplementary Fig. 24).

Discussion

Using a targeted metabolomics approach aimed at identifying plasma metabolites the levels of which predict risk of CVD in subjects, we have identified a novel pathway linking dietary lipid intake, intestinal microflora and atherosclerosis (Fig. 6). The pathway identified (dietary PC/choline → gut-flora-formed TMA → hepatic-FMO-formed TMAO) represents a unique additional nutritional contribution to the pathogenesis of CVD that involves PC and choline metabolism, an obligate role for the intestinal microbial community, and regulation of surface expression levels of macrophage scavenger receptors known to participate in the atherosclerotic process. The pro-atherogenic gut-flora-generated metabolite TMAO is formed in a two-step process initiated by gut-flora-dependent cleavage of a trimethylamine species (for example, PC, choline, betaine) generating the precursor TMA, and subsequent oxidation by FMO3 and possibly other FMOs (Fig. 6). PC is by far the most abundant dietary source of choline in most humans. The present results indicate that both environmental exposure (dietary lipid from predominantly animal products) and microbial flora participate in TMAO formation and producing a pro-atherogenic macrophage phenotype. Although the present genetic studies also indicate a role for hepatic expression levels of one or more *Fmo* genes in both enhanced atherosclerotic plaque and decreased HDL levels in mice, the participation of *FMO* genes in human atherosclerosis and HDL cholesterol levels remains to be established. Strong associations between systemic TMAO levels and both angiographic measures of coronary artery atherosclerotic burden and cardiac risks were observed among subjects; however, no correlation was observed between plasma TMAO levels and HDL cholesterol levels in subjects. It remains to be determined whether genetic impairment in *FMO3* alone or in

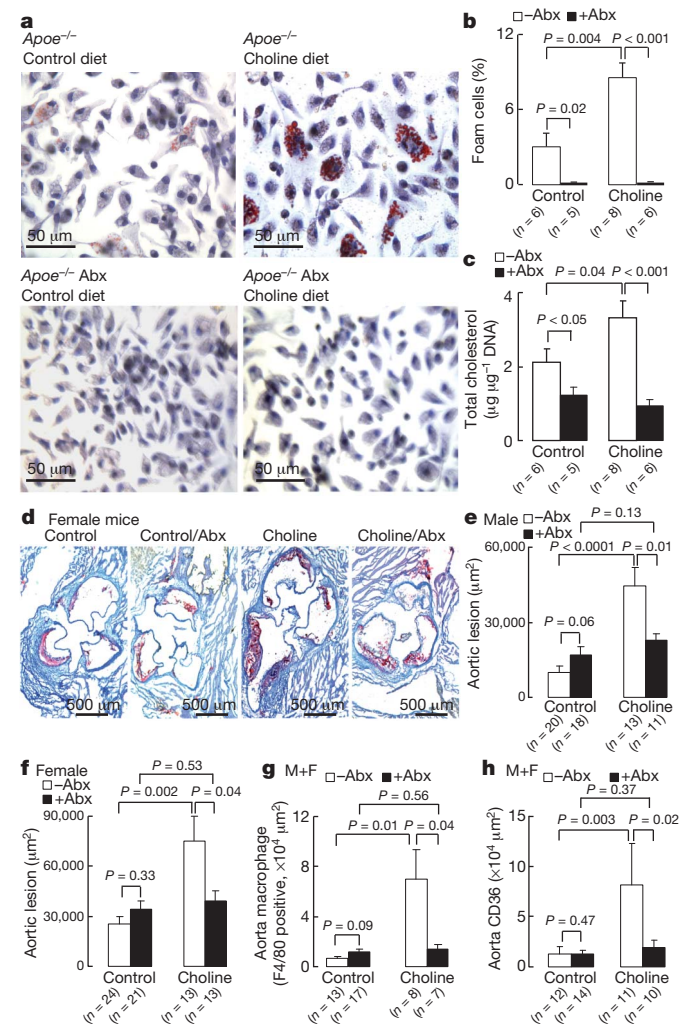


Figure 5 | Obligatory role of gut flora in dietary choline enhanced atherosclerosis. **a**, Choline supplementation promotes macrophage foam cell formation in a gut-flora-dependent fashion. C57BL/6J *Apoe*^{-/-} mice at time of weaning (4 weeks) were provided drinking water with or without broad-spectrum antibiotics (Abx), and placed on chemically defined diets similar in composition to normal chow (control diet, $0.08 \pm 0.01\%$ total choline, wt/wt) or normal chow with high choline (choline diet, $1.00\% \pm 0.01\%$ total choline, wt/wt). Resident peritoneal macrophages were recovered at 20 weeks of age. Typical images of Oil-red-O/haematoxylin-stained macrophages in each diet group are shown. **b**, Foam cell quantification from peritoneal macrophages recovered from mice in studies described in panel **a**. **c**, Macrophage cellular cholesterol content. **d**, Representative Oil-red-O/haematoxylin-stained aortic root sections from female C57BL/6J *Apoe*^{-/-} mice fed control and high-choline diets in the presence or absence of antibiotics. **e**, **f**, Aortic lesion area in 20 week old C57BL/6J *Apoe*^{-/-} mice off or on antibiotics and fed with control or choline diet. **g**, Aortic macrophage quantification with anti-F4/80 antibody staining. **h**, Quantification of the scavenger receptor CD36 in aorta within the indicated groups. Error bars represent s.e.m. from the indicated numbers of mice.

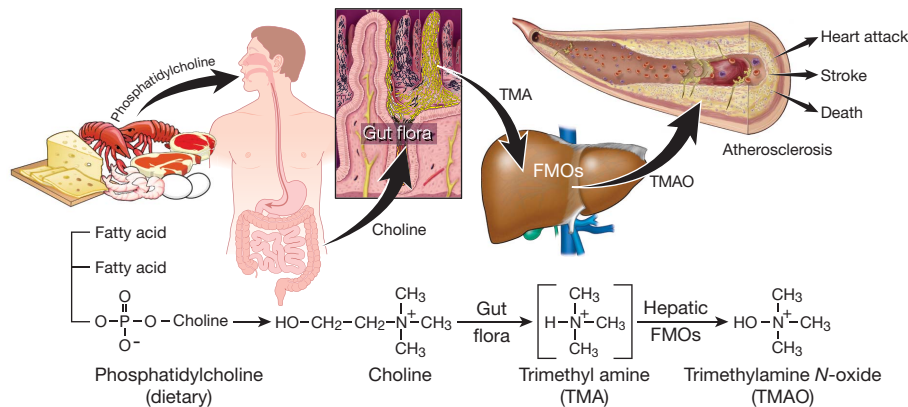


Figure 6 | Gut-flora-dependent metabolism of dietary PC and atherosclerosis. Schematic summary illustrating newly discovered pathway for gut-flora-mediated generation of pro-atherosclerotic metabolite from dietary PC.

combination with other *FMO* genes is protective for CVD. No phenotype other than the objectionable odour accompanying this disorder is known. In fact, individuals with trimethylaminuria often become vegans, as reducing the ingestion of dietary animal products rich in lipids decreases TMA production and the associated noxious odour. Little is also known about the biological functions of TMAO in humans. TMAO apparently serves as an osmolyte in the freeze-avoidance response of some species²¹. *In vitro* it can function as a small-molecule chaperone, affecting the folding and functioning of some proteins^{22,23}. In addition, TMAO and TMA accumulate in plasma of subjects on maintenance haemodialysis²⁴, raising the possibility that TMAO may contribute to the well-established enhanced CVD risk noted among subjects with end-stage renal disease.

Choline is an essential nutrient that is usually grouped within the vitamin B complex. Choline and its metabolite betaine are methyl donors, along with folate, and are metabolically linked to transmethylation pathways including synthesis of the CVD risk factor homocysteine. Deficiency in both choline and betaine have been suggested to produce epigenetic changes in genes linked to atherosclerosis^{25,26}, and acute choline and methionine deficiency in rodent models causes lipid accumulation in liver (steatohepatitis), heart and arterial tissues²⁷. Alternatively, some studies have reported an association between increased whole blood levels of total choline and cardiovascular disease^{28,29}. Few clinical studies have examined the relationship between choline intake and CVD³⁰, probably because accurate measures of the choline content of most foods has only recently become available¹⁴ (<http://www.nal.usda.gov/fnic/foodcomp/Data/Choline/Choln02.pdf>). The association between dietary choline (and alternative trimethyl-amine-containing species) and atherosclerosis will be complex because, as the present studies show, it will be influenced by inter-individual differences in the composition of the intestinal microflora.

The human intestinal microbial community is an enormous and diverse ecosystem with known functions in nutrition, gut epithelial cell health, and innate immunity³¹. Intestinal flora recently also has been implicated in the development of some metabolic phenotypes such as obesity and insulin resistance, as well as alterations in immune responses^{11,32–34}. To our knowledge, the present studies are the first to identify a direct link between intestinal microflora, dietary PC and CVD risk. These results indicate that an appropriately designed probiotic intervention may serve as a therapeutic strategy for CVD. Interestingly, production of TMAO can be altered by probiotic administration³⁵. Thus, in addition to the current clinical recommendation for a general reduction in dietary lipids, manipulation of commensal microbial composition may be a novel therapeutic approach for the prevention and treatment of atherosclerotic heart disease and its complications. The present studies also suggest a further novel treatment for atherosclerosis—blocking the presumed pathogenic biochemical pathway at the level of the gut flora through use of a non-systemically absorbed inhibitor.

METHODS SUMMARY

Plasma samples and associated clinical study data were identified in patients referred for cardiac evaluation at a tertiary care centre. All subjects gave written informed consent and the Institutional Review Board of the Cleveland Clinic approved all study protocols. Unbiased metabolic profiling was performed using LC/MS. Target analyte structural identification was achieved using a combination of LC/MS/MS, LC/MSⁿ, multinuclear NMR, GC/MS and choline isotope tracer feeding studies in mice as outlined in Methods. Statistical analyses were performed using R (version 2.10.1)³⁶. Intestinal microflora were suppressed by supplementation of drinking water with a cocktail of broad-spectrum antibiotics³⁷. Germ-free mice were purchased from Taconic SWGF. QTL analyses to identify atherosclerosis-related genes were performed on F2 mice generated by crossing atherosclerosis-prone C57BL/6J *Apoe*^{-/-} mice and atherosclerosis-resistant C3H/HeJ *Apoe*^{-/-} mice³⁸. mRNA expression was assayed by microarray analysis and real-time PCR. Aortic root lesion area in mice was quantified by microscopy after staining³⁹. Mouse peritoneal macrophages were collected by lavage for foam cell quantification and cholesterol accumulation assay. Surface protein levels of scavenger receptors CD36 and SR-A1 were determined by flow cytometry.

Full Methods and any associated references are available in the online version of the paper at www.nature.com/nature.

Received 29 July 2009; accepted 9 February 2011.

- Epstein, S. E. *et al.* The role of infection in restenosis and atherosclerosis: focus on cytomegalovirus. *Lancet* **348** (suppl. 1), S13–S17 (1996).
- Patel, P. *et al.* Association of *Helicobacter pylori* and *Chlamydia pneumoniae* infections with coronary heart disease and cardiovascular risk factors. *Br. Med. J.* **311**, 711–714 (1995).
- Danesh, J., Collins, R. & Peto, R. Chronic infections and coronary heart disease: is there a link? *Lancet* **350**, 430–436 (1997).
- Saikku, P. *et al.* Serological evidence of an association of a novel *Chlamydia*, TWAR, with chronic coronary heart disease and acute myocardial infarction. *Lancet* **332**, 983–986 (1988).
- O'Connor, C. M. *et al.* Azithromycin for the secondary prevention of coronary heart disease events—the WIZARD study: a randomized controlled trial. *J. Am. Med. Assoc.* **290**, 1459–1466 (2003).
- Cannon, C. P. *et al.* Antibiotic treatment of *Chlamydia pneumoniae* after acute coronary syndrome. *N. Engl. J. Med.* **352**, 1646–1654 (2005).
- Andraws, R., Berger, J. S. & Brown, D. L. Effects of antibiotic therapy on outcomes of patients with coronary artery disease: a meta-analysis of randomized controlled trials. *J. Am. Med. Assoc.* **293**, 2641–2647 (2005).
- Wright, S. D. *et al.* Infectious agents are not necessary for murine atherogenesis. *J. Exp. Med.* **191**, 1437–1442 (2000).
- Backhed, F., Ley, R. E., Sonnenburg, J. L., Peterson, D. A. & Gordon, J. I. Host-bacterial mutualism in the human intestine. *Science* **307**, 1915–1920 (2005).
- Turnbaugh, P. J. *et al.* An obesity-associated gut microbiome with increased capacity for energy harvest. *Nature* **444**, 1027–1031 (2006).
- Dumas, M. E. *et al.* Metabolic profiling reveals a contribution of gut microbiota to fatty liver phenotype in insulin-resistant mice. *Proc. Natl Acad. Sci. USA* **103**, 12511–12516 (2006).
- Cashman, J. R. *et al.* Biochemical and clinical aspects of the human flavin-containing monooxygenase form 3 (FMO3) related to trimethylaminuria. *Curr. Drug Metab.* **4**, 151–170 (2003).
- Al-Waiz, M., Mikov, M., Mitchell, S. C. & Smith, R. L. The exogenous origin of trimethylamine in the mouse. *Metabolism* **41**, 135–136 (1992).
- Zeisel, S. H., Mar, M. H., Howe, J. C. & Holden, J. M. Concentrations of choline-containing compounds and betaine in common foods. *J. Nutr.* **133**, 1302–1307 (2003).

15. Lang, D. H. *et al.* Isoform specificity of trimethylamine *N*-oxygenation by human flavin-containing monooxygenase (FMO) and P450 enzymes: selective catalysis by fmo3. *Biochem. Pharmacol.* **56**, 1005–1012 (1998).
16. Zhang, A. Q., Mitchell, S. C. & Smith, R. L. Dietary precursors of trimethylamine in man: a pilot study. *Food Chem. Toxicol.* **37**, 515–520 (1999).
17. Mitchell, S. C. & Smith, R. L. Trimethylaminuria: the fish malodor syndrome. *Drug Metab. Dispos.* **29**, 517–521 (2001).
18. Schadt, E. E. *et al.* An integrative genomics approach to infer causal associations between gene expression and disease. *Nature Genet.* **37**, 710–717 (2005).
19. Dolphin, C. T., Janmohamed, A., Smith, R. L., Shephard, E. A. & Phillips, I. R. Missense mutation in flavin-containing mono-oxygenase 3 gene, *FMO3*, underlies fish-odour syndrome. *Nature Genet.* **17**, 491–494 (1997).
20. Wang, S. S. *et al.* Identification of pathways for atherosclerosis in mice: integration of quantitative trait locus analysis and global gene expression data. *Circ. Res.* **101**, e11–e30 (2007).
21. Treberg, J. R., Wilson, C. E., Richards, R. C., Ewart, K. V. & Driedzic, W. R. The freeze-avoidance response of smelt *Osmerus mordax*: initiation and subsequent suppression of glycerol, trimethylamine oxide and urea accumulation. *J. Exp. Biol.* **205**, 1419–1427 (2002).
22. Devlin, G. L., Parfrey, H., Tew, D. J., Lomas, D. A. & Bottomley, S. P. Prevention of polymerization of M and Z α_1 -Antitrypsin (α_1 -AT) with trimethylamine *N*-oxide. Implications for the treatment of α_1 -AT deficiency. *Am. J. Respir. Cell Mol. Biol.* **24**, 727–732 (2001).
23. Song, J. L. & Chuang, D. T. Natural osmolyte trimethylamine *N*-oxide corrects assembly defects of mutant branched-chain α -ketoacid decarboxylase in maple syrup urine disease. *J. Biol. Chem.* **276**, 40241–40246 (2001).
24. Bain, M. A., Faull, R., Fornasini, G., Milne, R. W. & Evans, A. M. Accumulation of trimethylamine and trimethylamine-*N*-oxide in end-stage renal disease patients undergoing haemodialysis. *Nephrol. Dial. Transplant.* **21**, 1300–1304 (2006).
25. Dong, C., Yoon, W. & Goldschmidt-Clermont, P. J. DNA methylation and atherosclerosis. *J. Nutr.* **132**, 2406S–2409S (2002).
26. Zaina, S., Lindholm, M. W. & Lund, G. Nutrition and aberrant DNA methylation patterns in atherosclerosis: more than just hyperhomocysteinemia? *J. Nutr.* **135**, 5–8 (2005).
27. Salmon, W. D. & Newberne, P. M. Cardiovascular disease in choline-deficient rats. Effects of choline deficiency, nature and level of dietary lipids and proteins, and duration of feeding on plasma and liver lipid values and cardiovascular lesions. *Arch. Pathol.* **73**, 190–209 (1962).
28. Danne, O., Lueders, C., Storm, C., Frei, U. & Mockel, M. Whole blood choline and plasma choline in acute coronary syndromes: prognostic and pathophysiological implications. *Clin. Chim. Acta* **383**, 103–109 (2007).
29. LeLeiko, R. M. *et al.* Usefulness of elevations in serum choline and free F_2 -isoprostane to predict 30-day cardiovascular outcomes in patients with acute coronary syndrome. *Am. J. Cardiol.* **104**, 638–643 (2009).
30. Bidulescu, A., Chambless, L. E., Siega-Riz, A. M., Zeisel, S. H. & Heiss, G. Usual choline and betaine dietary intake and incident coronary heart disease: the Atherosclerosis Risk in Communities (ARIC) study. *BMC Cardiovasc. Disord.* **7**, 20 (2007).
31. Eckburg, P. B. *et al.* Diversity of the human intestinal microbial flora. *Science* **308**, 1635–1638 (2005).
32. Ley, R. E., Turnbaugh, P. J., Klein, S. & Gordon, J. I. Microbial ecology: human gut microbes associated with obesity. *Nature* **444**, 1022–1023 (2006).
33. Li, M. *et al.* Symbiotic gut microbes modulate human metabolic phenotypes. *Proc. Natl Acad. Sci. USA* **105**, 2117–2122 (2008).
34. Reigstad, C. S., Lunden, G. O., Felin, J. & Backhed, F. Regulation of serum amyloid A3 (SAA3) in mouse colonic epithelium and adipose tissue by the intestinal microbiota. *PLoS ONE* **4**, e5842 (2009).
35. Martin, F. P. *et al.* Probiotic modulation of symbiotic gut microbial–host metabolic interactions in a humanized microbiome mouse model. *Mol. Syst. Biol.* **4**, 157 (2008).
36. Rizzo, M. L. *Statistical Computing with R* (Chapman & Hall/CRC, 2008).
37. Rakoff-Nahoum, S., Paglino, J., Eslami-Varzaneh, F., Edberg, S. & Medzhitov, R. Recognition of commensal microflora by toll-like receptors is required for intestinal homeostasis. *Cell* **118**, 229–241 (2004).
38. Wang, S. *et al.* Genetic and genomic analysis of a fat mass trait with complex inheritance reveals marked sex specificity. *PLoS Genet.* **2**, e15 (2006).
39. Baglione, J. & Smith, J. D. Quantitative assay for mouse atherosclerosis in the aortic root. *Methods Mol. Med.* **129**, 83–95 (2006).

Supplementary Information is linked to the online version of the paper at www.nature.com/nature.

Acknowledgements We wish to thank E. Sehayek for discussions, L. W. Castellani for help with lipoprotein profile analysis, and F. McNally, M. Berk and M. Pepoy for technical assistance. This research was supported by National Institutes of Health grants R01 HL103866, P01 HL098055, P01HL087018-020001, P01 HL28481 and P01 HL30568. B.J.B. was supported by NIH training grant T32-DK07789. The clinical study GeneBank was supported in part by P01 HL076491-055328, R01 HL103931 and the Cleveland Clinic Foundation General Clinical Research Center of the Cleveland Clinic/Case Western Reserve University CTSA (1UL1R024989). Some of the laboratory studies (haemoglobin A1C, fasting glucose) in GeneBank were supported by R01 DK080732 and Abbott Diagnostics provided supplies for performance of some of the fasting lipid profile, glucose, creatinine, troponin I and hsCRP measured in GeneBank.

Author Contributions Z.W. performed metabolomics analyses, and biochemical, cellular, animal model and mass spectrometry studies. He assisted with statistical analyses, and assisted in both drafting and critical review of the manuscript. E.K., B.D. and J.D.S. assisted with performance of animal models and their analyses. B.S.L. synthesized d9-DPPC and assisted in metabolomics/mass spectrometry analyses. B.J.B., H.A. and A.J.L. performed the mouse eQTL experiments and analyses, and assisted in both drafting and critical review of the manuscript. A.J.L. provided some funding for the study. R.K., E.B.B., X.F. and Y.-M.C. performed mass spectrometry analyses of clinical samples. Y.W. performed statistical analysis. A.E.F. and P.S. helped with collection of human liver biopsy material and interpretation of biochemical and pathological examination of animal liver for steatosis. W.H.W.T. assisted in GeneBank study design and enrolment, as well as analyses of clinical studies and critical review of the manuscript. J.A.D. assisted in clinical laboratory testing for human clinical studies, animal model experimental design, and critical review of the manuscript. S.L.H. conceived of the idea, designed experiments, assisted in data analyses, the drafting and critical review of the manuscript, and provided funding for the study.

Author Information Reprints and permissions information is available at www.nature.com/reprints. The authors declare no competing financial interests. Readers are welcome to comment on the online version of this article at www.nature.com/nature. Correspondence and requests for materials should be addressed to S.L.H. (hazens@ccf.org).

METHODS

General procedures. Lipids were extracted by chloroform:methanol (2:1, v/v)⁴⁰. Cholesterol was quantified by GC/MS⁴¹. Triglyceride was quantified by GPO reagent set (Pointe Scientific)⁴². Cell DNA content was quantified by PicoGreen⁴³. RNA was isolated by TRIZOL reagent (Invitrogen) and RNeasy Mini Kit (Qiagen). All reagents were purchased from Sigma unless otherwise specified.

Research subjects. Plasma samples and associated clinical data were collected as part of two studies involving stable non-symptomatic subjects undergoing elective cardiac evaluations at a tertiary care centre. The first study, GeneBank, is a large well-characterized tissue repository with longitudinal data from subjects undergoing elective diagnostic left heart catheterization or elective coronary computed tomography angiography⁴⁴. The second study, BioBank, includes subjects undergoing cardiac risk factor evaluation/modification in a preventive cardiology clinic⁴⁵. CAD included adjudicated diagnoses of stable or unstable angina, myocardial infarction or angiographic evidence of $\geq 50\%$ stenosis of one or more epicardial vessels. PAD was defined as any evidence of extra-coronary atherosclerosis. Atherosclerotic CVD was defined as the presence of either CAD or PAD. All subjects gave written informed consent and the Institutional Review Board of the Cleveland Clinic approved all study protocols.

Discovery metabolomics analyses began with an unbiased search for plasma (fasting, EDTA purple top tube) analytes linked to CVD risk using a case-control design (Learning Cohort, $N = 50$ cases and 50 controls). Cases were randomly selected from GeneBank subjects who experienced a myocardial infarction, stroke or death over the ensuing 3-year period. An age- and gender-matched control group was randomly selected from GeneBank subjects that did not experience a CVD event. An independent non-overlapping Validation Cohort ($N = 25$ cases and 25 controls) was also from GeneBank. A third large ($N = 1,876$) independent study comprised of non-overlapping subjects then evaluated clinical associations of identified analytes. Approximately half ($N = 1,020$) of the subjects enrolled were from GeneBank and the remaining ($N = 856$) were from BioBank. Similar patient characteristics within each cohort and the combined cohort are observed, as shown in Supplementary Table 4a, b. The association of each PC metabolite and various cardiovascular phenotypes within each cohort (GeneBank and BioBank) are also similar (Supplementary Tables 4c–e). All subjects in the large independent clinical study had similar inclusion and exclusion criterion, negative cardiac enzymes (troponin I < 0.03 ng ml⁻¹) and no recent history of myocardial infarction or coronary artery bypass graft. Estimate of glomerular filtration rate was calculated using the MDRD formula⁴⁶. Fasting blood glucose, C reactive protein, troponin I and lipid profiles were measured on the Abbott ARCHITECT platform (Abbott Diagnostics).

Metabolomics analyses. Plasma proteins were precipitated with four volumes of ice-cold methanol and small-molecule analytes within supernatants were analysed after injection onto a phenyl column (4.6 \times 250 mm, 5 μ m Rexchrom Phenyl; Regis) at a flow rate of 0.8 ml min⁻¹ using a Cohesive HPLC interfaced with a PE Sciex API 365 triple quadrupole mass spectrometer (Applied Biosystems) with Ionics HSD+, EP10+, XT+ redesigned source and collision cell as upgrades in positive MS1 mode. LC gradient (LC1) starting from 10 mM ammonium formate over 0.5 min, then to 5 mM ammonium formate, 25% methanol and 0.1% formic acid over 3 min, held for 8 min, followed by 100% methanol and water washing for 3 min at a flow rate of 0.8 ml min⁻¹ was used to resolve analytes. Spectra were continuously acquired after the initial 4 min. Peaks within reconstructed ion chromatograms at 1 AMU increments were integrated and both retention times and m/z of analytes were used for statistical analyses.

Selection criteria for determining analytes of interest were based on the composite of MACE as the clinical phenotype, defined as incident myocardial infarction, stroke or death at 3 years, and included: (1) demonstration of a statistically significant difference between cases versus controls using a Bonferroni adjusted two sided t -test ($P < 0.05$); (2) evidence of a significant ($P < 0.05$) dose-response relationship between analyte level and clinical phenotype using Cochran-Armitage trend test; and (3) a minimal signal-to-noise ratio of 5:1 for a given analyte.

Chemical characterization of unknown metabolites. To chemically define the structures of the plasma analytes selected for further investigation (that is, analytes with m/z 76, 104 and 118 in positive MS1 mode), multiple approaches were used. Analytes of interest were isolated by HPLC, vacuum dried, re-dissolved in water and injected onto the same phenyl column with a distinct HPLC gradient (LC2, flow rate: 0.8 ml min⁻¹) starting from 0.2% formic acid over 2 min, then linearly to 18% acetonitrile containing 0.2% formic acid over 18 min and further to 100% acetonitrile containing 0.2% formic acid over 3 min. The targeted analytes were identified by their m/z and the appropriate fractions recovered. After removal of solvent, dry analytes were used for structural identification.

Samples analysed by GC/MS were derivatized using Sylon HTP kit (HMDS + TMCS + Pyridine (3: 1: 9), Supelco). Derivatization of TMAO and the plasma

analyte at m/z 76 also included initial reduction by titanium (III) chloride⁴⁷ and further reaction with 2,2,2-trichloroethylchloroformate⁴⁸. Analyses were performed on the Agilent Technologies 6890/5973 GC/MS in positive ion chemical ionization mode. The GC/MS analyses used a J&W Scientific DB-1 column (30 m, 0.25-mm inner diameter, 0.25- μ m film thickness) for separations.

Quantification of TMAO, choline and betaine. Stable isotope dilution LC/MS/MS was used for quantification of TMAO, choline and betaine. TMAO, choline and betaine were monitored in positive MRM MS mode using characteristic precursor-product ion transitions: m/z 76 \rightarrow 58, m/z 104 \rightarrow 60 and m/z 118 \rightarrow 59, respectively. The internal standards TMAO-trimethyl-d₉ (d₉-TMAO) and choline-trimethyl-d₉ (d₉-choline), were added to plasma samples before protein precipitation, and were similarly monitored in MRM mode at m/z 85 \rightarrow 68 and m/z 113 \rightarrow 69, respectively. Various concentrations of TMAO, choline and betaine standards and a fixed amount of internal standards were spiked into control plasma to prepare the calibration curves for quantification of plasma analytes. TMA was similarly quantified from acidified plasma by LC/MS/MS using MRM mode.

Aortic root lesion quantification. Apolipoprotein E knockout mice (C57BL/6J *Apoe*^{-/-}) were weaned at 4 weeks of age and fed with either standard chow control diet (Teklad 2018) or a custom diet comprised of normal chow supplemented with 0.5% choline (Teklad TD.07863), 1.0% choline (Teklad TD.07864) or 0.12% TMAO (Teklad TD.07865) for 16 weeks. Mice were anaesthetized with ketamine/xylazine before cardiac puncture to collect blood. Hearts were fixed and stored in 4% paraformaldehyde before frozen OCT sectioning and staining with Oil red O and haematoxylin. Aortic root lesion area was quantified as the mean value of six sections³⁹. Aortic sections were immunostained with rat anti-mouse F4/80 antibody (ab6640, Abcam) followed by goat anti-rat IgG-FITC antibody (sc-2011, Santa Cruz) and FITC-conjugated CD36 monoclonal antibody (Cayman Chemical) for F4/80 and CD36, respectively. Sections were mounted in Vectashield DAPI (H-1200, Vectashield) to take pictures under a Leica DMR microscope (W. Nuhsbaum) equipped with a Q Imaging Retiga EX camera. We used Image-Pro Plus Version 7.0 (MediaCybernetics) to integrate the positive staining area of F4/80 and CD36 in aorta.

Flow cytometry assays on scavenger receptors. Cell surface expression of scavenger receptors SR-A1 and CD36 were quantified on peritoneal macrophages from female mice by flow cytometry after immunostaining with fluorochrome-conjugated antibodies. Fluorescence intensity was quantified on a FACSCalibur flow cytometry instrument with FlowJo software (BD Biosciences). More than 10,000 total events were acquired to obtain adequate macrophages numbers. The following antibodies were used to stain macrophages: CD36 monoclonal antibody FITC (Cayman Chemical), anti-mouse SR-A1/MSRA1 (R&D Systems), goat anti-rat IgG-FITC (Santa Cruz Biotechnology), Alexa Fluor 647 anti-mouse F4/80 (eBioscience), Alexa Fluor 647 anti-mouse CD11b (eBioscience) and the isotype controls, Alexa Fluor 647 rat IgG2b (eBioscience), Alexa Fluor 647 rat IgG2a (eBioscience), normal mouse IgA-FITC (Santa Cruz). Cells were incubated with antibodies for 30 min at 4°C and washed with 0.1% BSA in PBS. Cells with double-positive staining for F4/80 and CD11b were gated as macrophage^{49–51} for the quantification of fluorescence intensity for CD36 and SR-A1 (Supplementary Fig. 20), with results normalized to F4/80.

eQTL studies. C57BL/6J *Apoe*^{-/-} (B6 *Apoe*^{-/-}) mice were purchased from the Jackson Laboratory and C3H/HeJ *Apoe*^{-/-} (C3H *Apoe*^{-/-}) mice were bred by backcrossing B6 *Apoe*^{-/-} to C3H/HeJ for 10 generations. F2 mice were generated by crossing B6 *Apoe*^{-/-} with C3H *Apoe*^{-/-} and subsequently intercrossing the F1 mice. Mice were fed Purina Chow containing 4% fat until 8 weeks of age, and then transferred to a Western diet (Teklad 88137) containing 42% fat and 0.15% cholesterol for 16 weeks until euthanasia at 24 weeks of age. Mouse atherosclerotic lesion area was quantified using standard methods³⁹. eQTL analyses were performed as previously described³⁸. Each individual sample was hybridized against the pool of F2 samples. Significantly differentially expressed genes were determined as previously described⁵². Expression data in the form of mean log ratios (mlratios) were treated as a quantitative trait in eQTL analysis using Rqt package for the R language and environment for statistical computing (<http://cran.r-project.org/>).

Germ-free mice and conventionalization studies. An antibiotic cocktail (0.5 g l⁻¹ vancomycin, 1 g l⁻¹ neomycin sulphate, 1 g l⁻¹ metronidazole, 1 g l⁻¹ ampicillin) previously shown to be sufficient to deplete all detectable commensal bacteria³⁷ was administered in drinking water ad libitum. In additional studies, 8-week-old female Swiss Webster germ-free mice (Taconic SWGF) underwent an oral (gavage) choline challenge (see later) immediately after their removal from their germ-free microisolator shipper. After the choline or PC challenge, the germ-free mice were placed in conventional cages with non-sterile C57BL/6J female mice to facilitate transfer of commensal organisms. Four weeks later, the conventionalized mice underwent a second choline or PC challenge.

- In vivo macrophage studies.** C57BL/6J mice or B6 *ApoE*^{-/-} mice were fed with either standard chow control diet (Teklad 2018) or a custom diet supplemented with 1.0% betaine (Teklad TD.08112), 1.0% choline (Teklad TD.07864), 0.12% TMAO (Teklad TD.07865) or 1.0% dimethylbutanol (DMB) supplemented in drinking water for at least 3 weeks. Elicited mouse peritoneal macrophages (MPMs) were harvested by peritoneal lavage with ice-cold PBS 3 days after i.p. injection of 1 ml 4% thioglycollate. Some studies with mice were performed using a custom diet with low but sufficient choline content (0.07% total; Teklad TD.09040) versus high-choline diet (1.0% total; Teklad TD.09041) in the presence or absence of antibiotics. Choline content of all diets was confirmed by LC/MS/MS.
- Foam cell staining.** Foam cells were identified by microscopy cultured peritoneal macrophages on glass coverslips after 6 h in RPMI 1640 medium supplemented with 3% lipoprotein-deficient serum. Cells were fixed with paraformaldehyde and stained with Oil red O/haematoxylin⁵³. Cells containing >10 lipid droplets were scored as foam cells⁵⁰. At least 10 fields and 500 cells per condition were counted.
- Real-time PCR.** Real-time PCR of *Cd36*, *Sr-a1* and flavin monooxygenases (mouse *Fmos*) was performed using Brilliant II SYBR Green qRT-PCR kit (Stratagene). The forward and reverse primers *Cd36*, *Gapdh*, *Sr-a1*, mouse *Fmos* and *F4/80* were synthesized by IDT based on sequences reported^{54–58}. RT-PCR of human FMOs was similarly performed using primers specific for the sequence of each of the indicated human FMOs.
- d9-DPPC synthesis and vesicle preparation.** d9-DPPC was synthesized by reacting 1,2-dipalmitoyl-sn-glycero-3-phosphoethanolamine (Genzyme Pharmaceuticals) with per-deuteromethyl iodide (CD₃I, Cambridge Isotope Laboratories)^{59,60}. The product was purified by preparative silica gel TLC and confirmed by both MS and NMR. Egg yolk lecithin (Avanti Polar Lipids) and d9-DPPC liposomes used for gavage feeding and i.p. injection of mice were prepared by the method of extrusion through polycarbonate filters⁶¹.
- Metabolic challenges in mice.** C57BL/6J mice were administered (gavage) unlabelled or the indicated stable-isotope-labelled choline or PC (egg yolk lecithin or d9-DPPC) using a 1.5-inch 20-gauge intubation needle. Choline challenge: gavage consisted of 150 μ l of 150 mM d9-choline. PC challenge: gavage or i.p. injection of 300 μ l 5 mg ml⁻¹ of unlabelled PC or labelled d9-DPPC. Mice were fasted 12 h before PC challenge. Plasma (50 μ l) was collected via the saphenous vein from mice at baseline and after gavage or i.p. injection time points.
- Statistical analysis.** Student's *t*-test and Wilcoxon rank sum test were employed to compare group means^{62,63}. Pearson correlation, Spearman rank correlation and Somers' Dxy correlation were used to investigate the correlation between two variables^{64,65}. Comparison of categorical measures between independent groups was done using χ^2 tests⁶⁶. Odds ratios and 95% confidence intervals for cardiovascular phenotypes (history of myocardial infarction, CAD, PAD, CVD and CAD+PAD) were calculated with R, version 2.10.1 (<http://www.r-project.org>), using logistic regression⁶⁷ with case status as the dependent variable and plasma analyte as independent variable. Trend tests in frequencies across quartiles were done using Cochran–Armitage trend tests⁶⁸. Levels of analytes were adjusted for traditional CAD risk factors in a multivariate logistic regression model including individual traditional cardiac risk factors (age, gender, diabetes, smoking, hypertension, lipids, CRP and estimated creatinine clearance) and medication usage (statin or other lipid-lowering agents, antihypertensive agents including angiotensin-converting-enzyme inhibitor, angiotensin-receptor blocking agent, diuretic, calcium-channel blocker or beta blocker, and aspirin or other platelet inhibitors).
40. Folch, J., Lees, M. & Sloane Stanley, G. H. A simple method for the isolation and purification of total lipides from animal tissues. *J. Biol. Chem.* **226**, 497–509 (1957).
 41. Robinet, P., Wang, Z., Hazen, S. L. & Smith, J. D. A simple and sensitive enzymatic method for cholesterol quantification in macrophages and foam cells. *J. Lipid Res.* **51**, 3364–3369 (2010).
 42. Millward, C. A. *et al.* Genetic factors for resistance to diet-induced obesity and associated metabolic traits on mouse chromosome 17. *Mamm. Genome* **20**, 71–82 (2009).
 43. Ahn, S. J., Costa, J. & Emanuel, J. R. PicoGreen quantitation of DNA: effective evaluation of samples pre- or post-PCR. *Nucleic Acids Res.* **24**, 2623–2625 (1996).
 44. Wang, Z. *et al.* Protein carbamylation links inflammation, smoking, uremia and atherogenesis. *Nature Med.* **13**, 1176–1184 (2007).
 45. Nicholls, S. J. *et al.* Lipoprotein (a) levels and long-term cardiovascular risk in the contemporary era of statin therapy. *J. Lipid Res.* **51**, 3055–3061 (2010).
 46. Stoves, J., Lindley, E. J., Barnfield, M. C., Burniston, M. T. & Newstead, C. G. MDRD equation estimates of glomerular filtration rate in potential living kidney donors and renal transplant recipients with impaired graft function. *Nephrol. Dial. Transplant.* **17**, 2036–2037 (2002).
 47. Barham, A. H. *et al.* Appropriateness of cholesterol management in primary care by sex and level of cardiovascular risk. *Prev. Cardiol.* **12**, 95–101 (2009).
 48. daCosta, K. A., Vrbanac, J. J. & Zeisel, S. H. The measurement of dimethylamine, trimethylamine, and trimethylamine *N*-oxide using capillary gas chromatography-mass spectrometry. *Anal. Biochem.* **187**, 234–239 (1990).
 49. Schledzewski, K. *et al.* Lymphatic endothelium-specific hyaluronan receptor LYVE-1 is expressed by stabilin-1⁺, F4/80⁺, CD11b⁺ macrophages in malignant tumours and wound healing tissue *in vivo* and in bone marrow cultures *in vitro*: implications for the assessment of lymphangiogenesis. *J. Pathol.* **209**, 67–77 (2006).
 50. Cailhier, J. F. *et al.* Conditional macrophage ablation demonstrates that resident macrophages initiate acute peritoneal inflammation. *J. Immunol.* **174**, 2336–2342 (2005).
 51. Kunjathoor, V. V. *et al.* Scavenger receptors class A-I/II and CD36 are the principal receptors responsible for the uptake of modified low density lipoprotein leading to lipid loading in macrophages. *J. Biol. Chem.* **277**, 49982–49988 (2002).
 52. Yang, X. *et al.* Tissue-specific expression and regulation of sexually dimorphic genes in mice. *Genome Res.* **16**, 995–1004 (2006).
 53. Zhou, J., Lhotak, S., Hilditch, B. A. & Austin, R. C. Activation of the unfolded protein response occurs at all stages of atherosclerotic lesion development in apolipoprotein E-deficient mice. *Circulation* **111**, 1814–1821 (2005).
 54. Miles, E. A., Wallace, F. A. & Calder, P. C. Dietary fish oil reduces intercellular adhesion molecule 1 and scavenger receptor expression on murine macrophages. *Atherosclerosis* **152**, 43–50 (2000).
 55. Westendorf, T., Graessler, J. & Kopprasch, S. Hypochlorite-oxidized low-density lipoprotein upregulates CD36 and PPAR γ mRNA expression and modulates SR-BI gene expression in murine macrophages. *Mol. Cell. Biochem.* **277**, 143–152 (2005).
 56. Rasooly, R., Kelley, D. S., Greg, J. & Mackey, B. E. Dietary *trans* 10, *cis* 12-conjugated linoleic acid reduces the expression of fatty acid oxidation and drug detoxification enzymes in mouse liver. *Br. J. Nutr.* **97**, 58–66 (2007).
 57. Zhang, J. & Cashman, J. R. Quantitative analysis of *FMO* gene mRNA levels in human tissues. *Drug Metab. Dispos.* **34**, 19–26 (2006).
 58. de Vries, T. J., Schoenmaker, T., Hooibrink, B., Leenen, P. J. & Everts, V. Myeloid blasts are the mouse bone marrow cells prone to differentiate into osteoclasts. *J. Leukoc. Biol.* **85**, 919–927 (2009).
 59. Chen, F. C. M. & Benoiton, L. N. A new method of quaternizing amines and its use in amino acid and peptide chemistry. *Can. J. Chem.* **54**, 3310–3311 (1976).
 60. Morano, C., Zhang, X. & Fricker, L. D. Multiple isotopic labels for quantitative mass spectrometry. *Anal. Chem.* **80**, 9298–9309 (2008).
 61. Greenberg, M. E. *et al.* The lipid whisker model of the structure of oxidized cell membranes. *J. Biol. Chem.* **283**, 2385–2396 (2008).
 62. Gauvreau, K. & Pagano, M. Student's *t*-test. *Nutrition* **9**, 386 (1993).
 63. Wijnand, H. P. & van de Velde, R. Mann–Whitney/Wilcoxon's nonparametric cumulative probability distribution. *Comput. Methods Programs Biomed.* **63**, 21–28 (2000).
 64. Gaddis, M. L. & Gaddis, G. M. Introduction to biostatistics: part 6, correlation and regression. *Ann. Emerg. Med.* **19**, 1462–1468 (1990).
 65. Deichmann, M. *et al.* S100- β , melanoma-inhibiting activity, and lactate dehydrogenase discriminate progressive from nonprogressive American Joint Committee on Cancer stage IV melanoma. *J. Clin. Oncol.* **17**, 1891–1896 (1999).
 66. Goodall, C. M., Stephens, O. B. & Moore, C. M. Comparative sensitivity of survival-adjusted chi-square and normal statistics for the mutagenesis fluctuation assay. *J. Appl. Toxicol.* **6**, 95–100 (1986).
 67. Traissac, P., Martin-Prevel, Y., Delpeuch, F. & Maire, B. Logistic regression vs other generalized linear models to estimate prevalence rate ratios. *Rev. Epidemiol. Sante Publique* **47**, 593–604 (1999).
 68. Gautam, S. Test for linear trend in 2 \times K ordered tables with open-ended categories. *Biometrics* **53**, 1163–1169 (1997).